



Thermal Decomposition of Hydroxylammonium Nitrate: ReaxFF Training Set Development for Molecular Dynamics Simulations

Daniel D. Depew^{*}, Joseph J. Wang[†], and Shehan M. Parmar[‡]
University of Southern California, Los Angeles, CA 90089

Steven D. Chambreau[§]
ERC, Inc., Edwards Air Force Base, CA 93524

Dmitry Bedrov[¶]
University of Utah, Salt Lake City, UT 84112

Adri van Duin^{||}
Pennsylvania State University, University Park, PA 16802

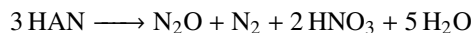
Ghanshyam L. Vaghjiani^{**}
Air Force Research Laboratory, AFRL/RQRS, Edwards Air Force Base, CA 93524

A ReaxFF reactive force field training set has been developed for the thermal decomposition of hydroxylammonium nitrate (HAN). The training set consists of geometries, partial atomic charges, and energy barriers for a number of reactions relevant to HAN thermal decomposition. Geometries and partial atomic charges were calculated in both the gas phase and in solution at the M06-2X/aug-cc-pVTZ level of theory. The SMD-GIL solvent model was used to approximate a high concentration of HAN in solution. Transition states for elementary reactions were found at the GIL/ ω B97X-D/6-311++G level of theory. An important autocatalytic pathway for the regeneration of HONO in HAN decomposition is discussed. The training set from this work can be used to train a ReaxFF force field capable of conducting reactive molecular dynamics simulations of HAN thermal decomposition.**

I. Introduction

Hydroxylammonium nitrate (HAN) has been of interest recently as a component of novel green propellants. The high energy density and low vapor toxicity of HAN makes it an attractive candidate to replace hydrazine as a monopropellant [1]. It has been suggested that the hydrogen bonding which occurs due to the hydroxyl group on the cation decreases the vapor pressure, as well as enhancing water miscibility and increasing the boiling point [2]. HAN in the solid state is unstable, but it is readily dissolved in H₂O, where it can dissolve at a concentration of up to 95% by weight with a stoichiometry of up to six HAN molecules to one H₂O molecule [3, 4]. At high concentrations, the properties of HAN-water mixtures resemble the properties of molten salts [2].

The thermal decomposition of HAN has been studied at length both experimentally and theoretically. Oxley and Brower proposed two global reactions based on experimental observations [5]:



^{*}Graduate Student, Department of Astronautical Engineering, 854B Downey Way, Los Angeles, CA 90089, AIAA Student Member.

[†]Professor, Department of Astronautical Engineering, 854B Downey Way, Los Angeles, CA 90089, AIAA Associate Fellow.

[‡]Undergraduate Student, Department of Astronautical Engineering, 854B Downey Way, Los Angeles, CA 90089, AIAA Student Member

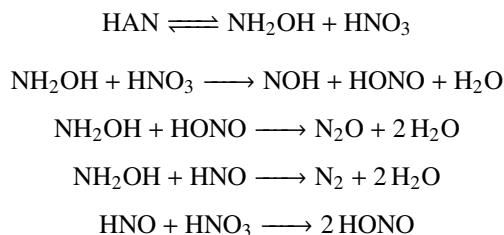
[§]Research Scientist, ERC, Inc., Edwards Air Force Base, California 93524.

[¶]Associate Professor, Department of Materials Science & Engineering, 122 S. Central Campus Drive, Salt Lake City, UT 84112.

^{||}Professor, Department of Mechanical and Nuclear Engineering, 240 Research East Building, University Park, PA 16802.

^{**}Senior Research Chemist, In-Space Propulsion Branch, Rocket Propulsion Division, Aerospace Systems Directorate, Air Force Research Laboratory, AFRL/RQRS, Edwards Air Force Base, CA 93524.

Their commonly cited reactions are composed of both elementary and complex reactions:



Later experiments have also observed NO and NO₂ products [2, 6]. The advancement in computational chemistry methods opened up the possibility of exploring elementary reaction steps in considerable detail. Raman et al. performed B3LYP/6-311G(2d,d,p) and CBS-QB3 calculations of geometries and energies, respectively, for hypothesized HNO₂ autocatalytic and scavenging reactions in aqueous nitric acid using the IEF-PCM implicit solvation model [7]. They proposed an intermediate of NH₃ONO⁺ in the scavenging reaction of nitrous acid. Izato et al. performed a similar study of aqueous HAN using the ω B97X-D/6-311++G(d,p) level of theory for geometries and frequencies, again with CBS-QB3 energies and PCM solvation model [8]. They identified reaction pathways for the initial decomposition from the ion-neutral reaction of NH₃OH⁺ with HNO₃, the neutral-neutral reaction of NH₃O with HNO₃, and two self-decomposition mechanisms for HNO₃. These mechanisms all produce HNO₂, HNO, and H₂O and their relative importance depends on the initial concentrations of the species. Additionally, six catalytic mechanisms were proposed, with no clear autocatalytic pathway identified.

Zhang and Thynell built upon previous studies to develop a detailed mechanism for the thermal decomposition of aqueous HAN [9]. They used the ω B97X-D/6-311++G** level of theory, while using the newer SMD solvation model instead of IEF-PCM. In addition to reactions which lead to the formation of HONO and HNO, and HONO scavenging/autocatalytic reactions, they included reactions describing the homolytic dissociation of several species to explain the evolution of NO₂ and NH₂O. They proposed that autocatalysis is not primarily due to the accumulation of nitrous acid as previously hypothesized, but rather due to the rise of solution acidity [9].

Atomistic modeling using molecular dynamics (MD) has proven a valuable tool to investigate time and length scales not accessible by quantum mechanical and experimental techniques. In this work, we extend previous theoretical investigations of HAN in order to develop a training set of data which can be used to parametrize a ReaxFF force field capable of modeling HAN thermal decomposition. The paper is organized as follows: Section II provides background into the ReaxFF methodology and describes the DFT techniques used, Section III presents in detail some of the density functional theory (DFT) data generated for the training set, and Section IV contextualizes the data and discusses future work.

II. Theoretical Methods

A. ReaxFF: Reactive Molecular Dynamics

ReaxFF is a formalism designed to model reactive and non-reactive interactions between atoms [10]. Fundamentally, it is a bond-order potential with application to molecular dynamics (MD) simulations. ReaxFF differs from potentials used in classical MD methods in that it does not use a fixed connectivity assignment between atoms, but instead allows bonds to form and break implicitly based on the chemical environment. The polarization of charges within molecules is considered via the electronegativity equilibration method (EEM) developed by Mortier et al. to calculate partial atomic charges [11]. In this way, ReaxFF can model both covalent and electrostatic interactions, enabling the study of reactions in a dynamic environment. An excellent overview of ReaxFF is given in [12], which highlights the evolution of the method since it was first introduced by Van Duin in 2001 [10].

The total potential energy of a system in ReaxFF is the sum of a number of partial energy terms as shown in Eq. 1.

$$E_{\text{system}} = E_{\text{bond}} + E_{\text{over}} + E_{\text{under}} + E_{\text{val}} + E_{\text{tors}} + E_{\text{lp}} + E_{\text{coa}} + E_{\text{conj}} + E_{\text{H-bond}} + E_{\text{vdWaals}} + E_{\text{Coulomb}} \quad (1)$$

Nomenclature for these terms is adopted from [13], where their full functional forms are described in the supporting information of that paper. All terms except for E_{vdWaals} and E_{Coulomb} are functions of bond order. The bond order

BO_{ij} between a pair of atoms is a function of interatomic distance r_{ij} and is further decomposed into contributions from sigma, pi, and double pi bonds as in Eq. 3.

$$BO_{ij} = BO_{ij}^{\sigma} + BO_{ij}^{\pi} + BO_{ij}^{\pi\pi} \quad (2)$$

$$= \exp \left[p_{bo,1} \left(\frac{r_{ij}}{r_0} \right)^{p_{bo,2}} \right] + \exp \left[p_{bo,3} \left(\frac{r_{ij}}{r_0} \right)^{p_{bo,4}} \right] + \exp \left[p_{bo,5} \left(\frac{r_{ij}}{r_0} \right)^{p_{bo,6}} \right] \quad (3)$$

The p_{bo} and r_0 terms are empirical parameters which are included in the force field. The form of Eq. 3 can capture the long-distance covalent interactions found in transition states, but it also leads to overcoordination of non-bonded neighbors. Correcting for overcoordination, the corrected bond orders are then used to calculate other terms in Eq. 1. The bond energy E_{bond} can then be computed directly from bond order and additional empirical parameters. If the corrected bond order is greater than the number of bonding electrons, then the atom is overcoordinated and an energy penalty E_{over} is imposed, taking into account the atom's number of lone pairs. Similarly, an undercoordinated atom which exhibits pi bond character with neighboring atoms will have an energy contribution E_{under} due to resonance of the π -electron. The E_{val} and E_{tors} energies account for valence and torsional angle strains, respectively. ReaxFF assumes each atom type has an optimal number of lone pairs, imposing an energy penalty E_{lp} as lone pairs are broken up with increasing coordination. Conjugation effects are considered for three body (E_{coa}) and four body (E_{conj}) conjugation. The three body conjugation was added later [14] in particular to describe increased stability due to $-\text{NO}_2$ group conjugation. The hydrogen bond term E_{Hbond} is also bond-order dependent. The non-bonding terms $E_{vdWaals}$ and $E_{Coulomb}$ specify energy contributions from dispersive and electrostatic interactions and are calculated between all atom pairs regardless of connectivity and bond order, leading to independence of the bonding and non-bonding terms. A shielding term is applied to these non-bonding interactions to limit excessive influence at short distances.

B. Training of ReaxFF Parameters

Each of the terms in Eq. 1 is a function of multiple empirical parameters in addition to the bond order for the bonding terms. Some empirical parameters have a direct physical interpretation, while others are simply prefactors or exponential factors. In the literature and in this work, the terms "force field" and "parameter set" are interchangeable and refer to the text file read in by the ReaxFF program which contains the many empirical parameters used in the interatomic potential functions. The force field parameters must be fit to a training set of quantum chemical (QC) or experimental data applicable to the system of interest. Since 2005, parameter sets have been developed to describe a number of elements on the periodic table. As these parameter sets were derived from the stable 2005 ReaxFF_{RDX} formalism, Senftle et al. depict the different parametrizations as "branches" on a development tree [12]. Splitting the development into branches works not only to characterize the parametrizations which have been implemented, but also to emphasize that generally, transferring parameters across branches will not work without extensive refitting. The ReaxFF parameters were designed to be general enough to describe interactions across many chemical environments—including ones for which it had not been explicitly trained—however this transferability is limited. For instance, the 2008-C/H/O combustion force field can describe gas-phase water molecules correctly but fails to describe water in the liquid phase, which led to the development of the aqueous branch [15].

Data included in a ReaxFF training set consist of: geometries, partial atomic charges, cell parameters (for bulk solids), and energies. In the geometries section, equilibrium bond lengths, valence angles, and torsion angles can be specified for any combination of atoms in a given structure. Partial atomic charges are given on a per-atom basis in the structure. By default, the charge equilibration scheme in ReaxFF assumes the system is charge-neutral, however, an effective "molecular charge" can be specified. The cell parameters section accepts equilibrium lattice parameters for the bulk solid. The section for energies is the most general and also provides the most flexibility for incorporating experimental and QC data. Each entry in the energies section contains references to two structures such that the energy difference between them can be compared to a specified value. Energies of reaction can be included by specifying the difference in energy between reactants and products for a particular reaction. Additionally, barrier heights or portions of the potential energy surface of a specific pathway can be included using this scheme.

The force field training procedure is an optimization problem, where the variables are the parameters in the force field and objective function is the sum of the squared differences (i.e. error) between values of properties entered in the training set and the values as determined by ReaxFF. The size and nonlinearity of this optimization problem—in addition to the large number of empirical parameters in the force field—subjects ReaxFF training to the possibility of overparametrization. Inclusion of too many specific or too highly-weighted properties may restrict transferability of the

force field. Additionally, a small change to the force field parameters may have large unintended consequences. For this reason, extensive cross-validation and testing is necessary to ensure the applicability of a training set.

The analogy of the ReaxFF development “tree” is appropriate, as major branches should contain highly weighted portions of the training set dedicated to fundamental properties of bonding interaction common to all sub-branches. For example, the original 2001 ReaxFF hydrocarbon force field included bond dissociation energies for ethane (H_3CCH_3), ethylene (H_2CCH_2), and ethyne (HCCH) as part of a general description of C–C single, double, and triple bonds, respectively [10]. The foundational ReaxFF publications have applicability to high energy reactions, as ReaxFF was first developed for hydrocarbons. This original publication included numerous bond dissociations, torsional barriers, and barriers to isomerization for small hydrocarbons. Strachan et al. developed a ReaxFF description of RDX decomposition, which is the current baseline for high-energy studies containing nitramines or similar species [14, 16]. It again focused on elementary bond, angle, and torsion barriers and energies for a number of small C/H/O/N species. Many isomerization energies were given as energy differences instead of training on the full potential energy surface. Finally, partial atomic charges were trained for select molecules, which included water, NH_3 , HONO, RDX, HOCH_2NH_3 , urea, and alanine. Chenoweth et al. extended the previous training sets to create a force field specially tuned for hydrocarbon combustion [17]. This involved adding a number of elementary reaction steps and mechanisms including radical chemistry. The potential energy surface for some of these reactions was incorporated into the training set. More recent work on the hypergolic ignition of ionic liquids with nitric acid focused on characterizing intermediate species in the combustion [18, 19]. They built upon the existing high energy training set to add reaction pathways specific to their system, incorporating the potential energy surface of several intermediate reactions which were not well characterized. Nearly all of the QC data in these studies were generated from DFT calculations using the B3LYP hybrid functional.

C. Density Functional Theory Methods

All calculations were done in GAMESS, an open source general-purpose electronic structure code which contains implementations for a number of semi-empirical, DFT, and *ab initio* methods [20]. The SMD solvation model was used for solution-phase calculations. While previous studies of HAN decomposition used a water solvent [8, 9], the high concentration of HAN in monopropellant applications results in behavior resembling a molten salt [2]. Consequently the “generic ionic liquid” parameters of Bernales et al. were used as the solvent [21], which we refer to as the SMD-GIL model. In the time since ReaxFF was introduced, significant advancement has been achieved in DFT methods at higher rungs of Jacob’s ladder [22], leading to the possibility of training ReaxFF parameters on energies obtained using more sophisticated and accurate techniques. All transition states and their associated reactants and products were optimized using the $\omega\text{B97X-D}$ exchange correlation functional with the 6-311++G** basis set [23]. The $\omega\text{B97X-D}$ functional is a dispersion-corrected hybrid functional and has been used with the 6-311++G** basis set in previous theoretical studies of HAN decomposition [8, 9]. For all other calculations, the M06-2X exchange correlation functional was used with Dunning’s aug-cc-pVTZ basis set [24, 25]. The M06-2X functional is well-characterized for general-purpose use. While this functional is not explicitly dispersion corrected, it has been successful for dispersion interactions [26]. Additionally, the aug-cc-pVTZ basis set is large and augmented with diffuse orbitals, useful for these interactions. Calculations of partial atomic charges were performed using the Geodesic scheme [27]. Although the Mulliken charge scheme is by far the most-used scheme for ReaxFF training, Rigby and Izgorodina found that it was highly basis set dependent when applied to ionic liquids and demonstrated much better performance with the Connolly and Geodesic schemes [28].

III. Results

A. HAN Structures, Geometries, and Charges

In order to simulate thermal decomposition of HAN, a ReaxFF force field must be able to produce a stable HAN solution at high concentration. For this reason, the NH_3OH^+ and NO_3^- ions and their corresponding neutral species were studied in detail at the GIL/M06-2X/aug-cc-pVTZ level of theory. Optimized geometries and partial atomic charges are shown for these isolated species in Figure 1. The –OH group on the NH_3OH^+ cation is nearly neutral, while the – NH_3 group contains a net charge of approximately +1. The central nitrogen on the NO_3^- anion has a charge of +1 and the remaining negative charge is uniformly distributed among the O atoms. As the NO_3^- anion is protonated to HNO_3 , approximately half of the proton’s charge is distributed to the O atoms. This is accompanied by a reduction of positive charge on the central N atom as well.

In the gas phase, an isolated $\text{NH}_3\text{OH}^+/\text{NO}_3^-$ ion pair does not exist, as the interaction energy is not strong enough to

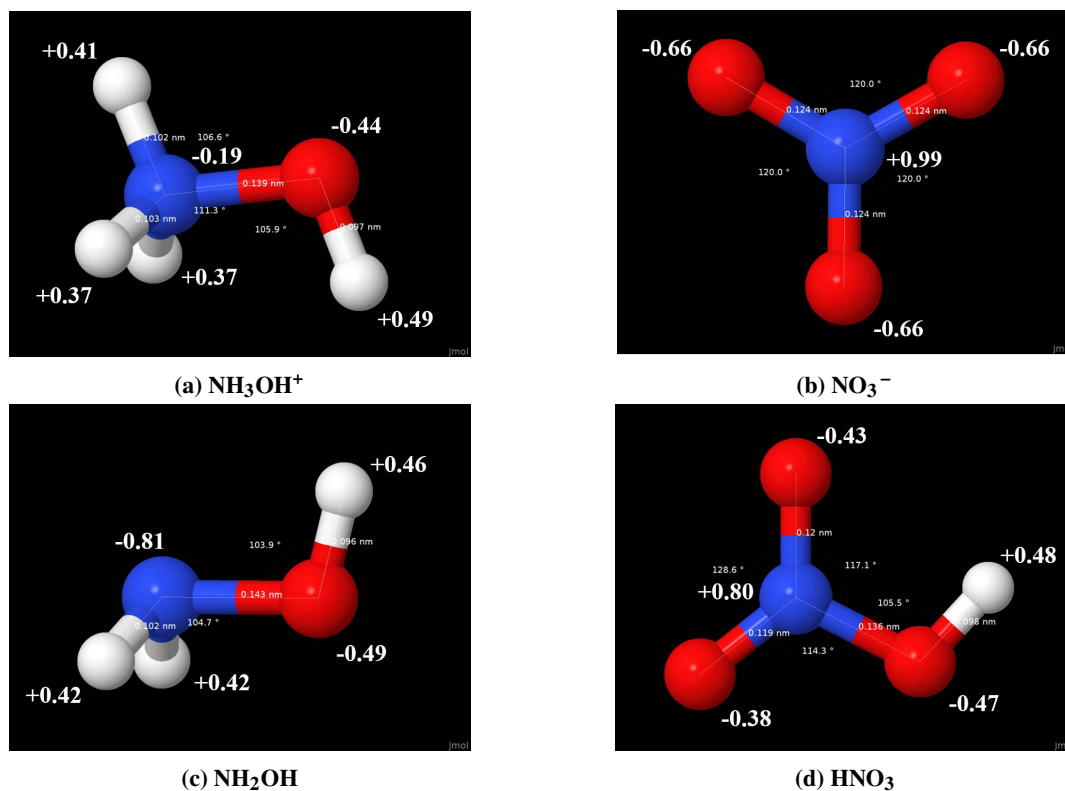


Fig. 1 Optimized geometries and partial atomic charges for HAN ions and neutrals at the GIL/M06-2X/aug-cc-pVTZ level of theory

overcome proton transfer from one of the $-\text{NH}_3$ protons to the NO_3^- anion. This creates a structure of hydrogen-bonded hydroxylamine (NH_2OH) and nitric acid (HNO_3). Four optimized structures were found and are shown in Figure 2. The energies of these structures relative to the isolated neutral species are listed in Table 1. Structures 1-3 have been previously identified in [29] and [9]. The energy differences between the structures in this study are very similar to previous results which used a water solvent. The lowest-energy Structure 1 maximizes hydrogen bonding with both the O atom and N atom of hydroxylamine forming H bonds with sites on the nitric acid molecule. Structure 4 differs from Structure 2 only by rotation of the $-\text{OH}$ group of hydroxylamine to be *cis* relative to the $-\text{NH}_2$ group. There is a 2.6 kcal/mol difference in electronic energy between these structures.

Isolated HAN exists as ions when in solution. Four optimized structures containing ion pairs were found when applying the SMD-GIL model, shown in Figure 3. Table 2 contains the energies of these structures relative to isolated neutral species in solution—that is, $\text{NH}_2\text{OH}(l)$ and $\text{HNO}_3(l)$. The first three structures were also identified by [9] and energy differences are again in good agreement. Notably, Structures 1-3 in the gas phase appear to have a one-to-one correspondence to Structures 1-3 in the condensed phase. Examining the differences in energy among them clearly shows that the GIL solvent stabilizes the ions in the presence of hydrogen bonding between the anion and the $-\text{NH}_3$

Structure Number	Energy (kcal/mol)
1	-16.2
2	-12.6
3	-10.4
4	-10.0

Table 1 Electronic energies of Structures in Fig. 2 relative to isolated $\text{NH}_2\text{OH}(g) + \text{HNO}_3(g)$

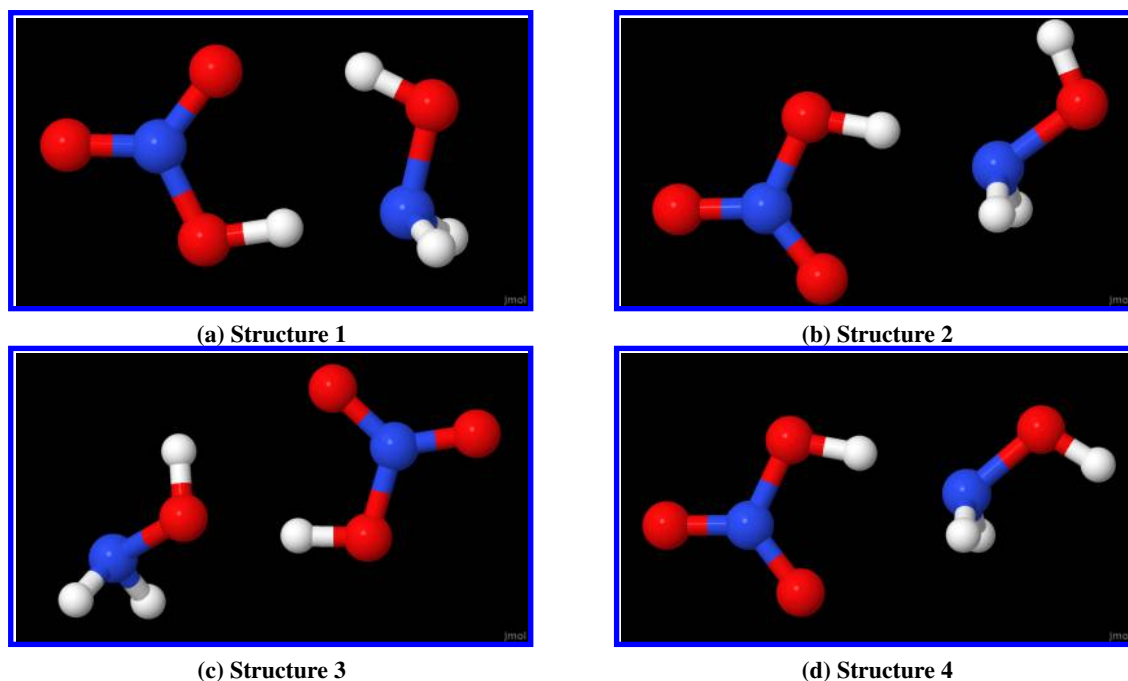
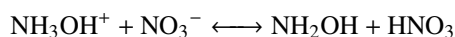


Fig. 2 Optimized gas-phase geometries for pairs of NH_2OH and HNO_3 at the M06-2X/aug-cc-pVTZ level of theory

group of the cation. The partial atomic charges for the lowest-energy structure were then compared to the isolated ions. The net charge on the cation and anion are reduced from unity to ± 0.83 , respectively, indicating a small amount of charge transfer.

Prior to decomposition, the stable HAN solution is assumed to be an equilibrium mixture of mostly ions with some neutral species:



In order for ReaxFF to model this equilibrium, it must be able to represent accurately the energy changes due to proton transfer in HAN. A relaxed potential energy surface (PES) scan was performed for HAN proton transfer as follows: on the minimum-energy Structure 1 (see Fig. 3a), a distance constraint is imposed on the N atom of NH_3OH^+ with respect to the H atom which is hydrogen bonded to the NO_3^- . By fixing this N–H distance on NH_3OH^+ to successively longer distances while relaxing the rest of the structure, the anion is protonated to yield HNO_3 . The electronic energies from this PES scan are plotted in Fig. 4 up to an N–H distance of 2.0\AA . No transition state is observed, and extending the N–H distance to infinite length yields the energy of reaction $\Delta E_{r,xn}$ for this proton transfer as $+21.9\text{ kcal/mol}$, which corresponds to the value for Structure 1 from Table 2.

Structure Number	Energy (kcal/mol)
1	-21.9
2	-17.0
3	-10.3
4	-17.8

Table 2 Electronic energies of Structures in Fig. 3 relative to isolated $\text{NH}_2\text{OH}(l) + \text{HNO}_3(l)$

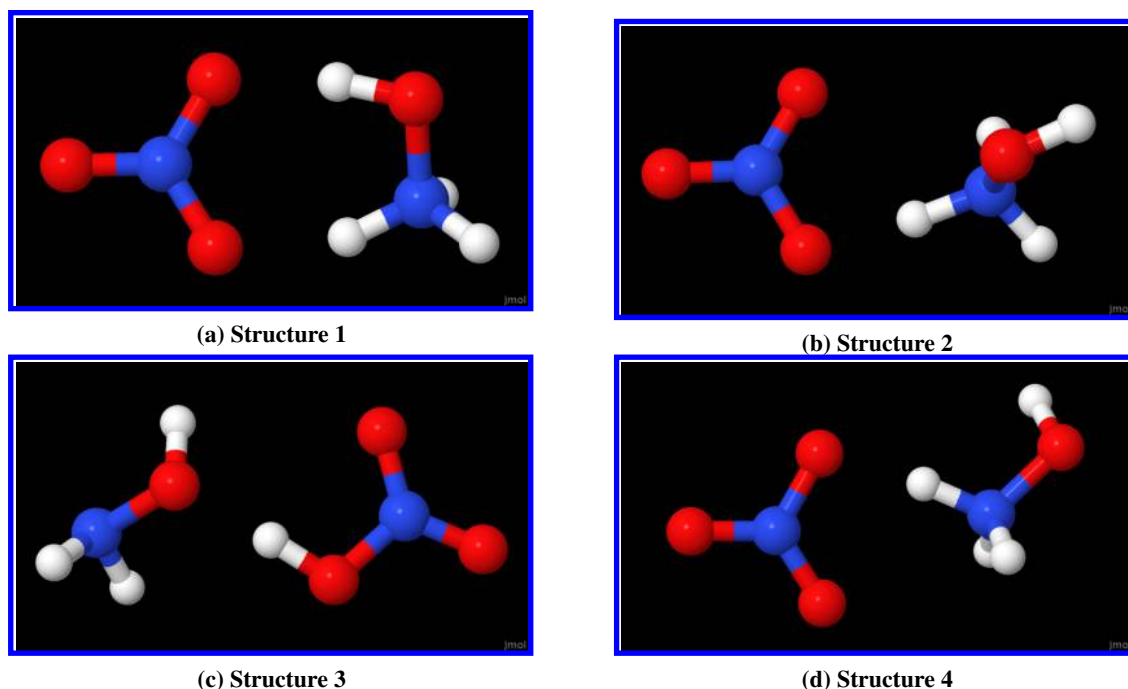


Fig. 3 Optimized condensed-phase geometries for pairs of NH_3OH^+ and NO_3^- at the GIL/M06-2X/aug-cc-pVTZ level of theory

B. Investigation of Decomposition Pathways

While the detailed mechanism contains a number of potential decomposition pathways, the autocatalytic pathways involving HONO scavenging-regeneration are the most important. The results in this paper focus on a particular free radical pathway to nitrous acid (HONO) regeneration which was identified previously in [7] and [9]. A series of steps for this pathway follows:



In this pathway, the production of NO_2 radicals is followed by a series of hydrogen abstractions by the radicals to produce HONO. This corresponds to a global reaction which generates 3 additional HONO molecules:



With the exception of the unimolecular dissociation reactions R2 and R6, transition state geometries were identified for each of R1-R7 at the GIL/ ω B97X-D/6-311++G** level of theory. A vibrational analysis was performed to confirm that each transition state contained exactly one imaginary frequency. Intrinsic reaction coordinate calculations connected the transition states to their corresponding reactant and product structures.

Table 3 summarizes the barrier heights and reaction energies in reactions R1-R7. Here, the barrier height ΔE_f is defined as the difference in electronic energy between the transition state and the reactants, if the transition state exists. Similarly, the reaction energy ΔE_{rxn} is defined as the difference in electronic energy between the products and the reactants. Note that the electronic energies are reported here and not the Gibbs free energies, as ReaxFF does not incorporate temperature dependence in its training. Geometries for each transition state are depicted in Figure 5.

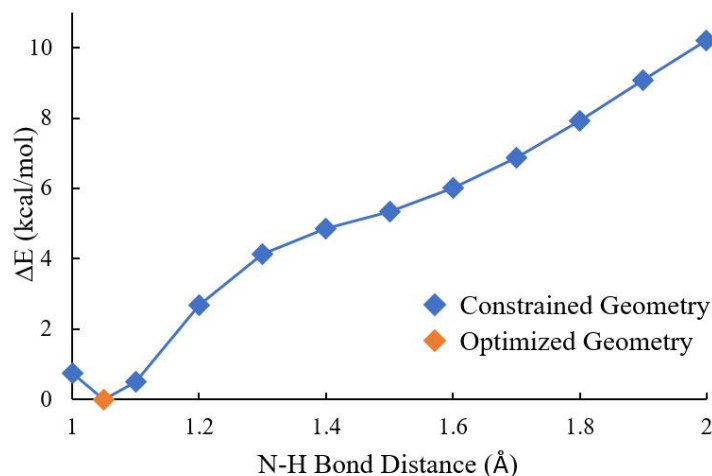


Fig. 4 Relaxed potential energy surface scan for proton transfer in $\text{NH}_3\text{OH}^+/\text{NO}_3^-$ ion pair at the GIL/M06-2X/aug-cc-pVTZ level of theory

IV. Discussion and Conclusion

A number of geometries, partial atomic charges, and structures relevant to modeling HAN were calculated using DFT methods. In addition, transition states were found for a large number of reactions which constitute various pathways for HAN thermal decomposition. The DFT-generated electronic energies for all reactions — in conjunction with the geometries and charges — compose a reference data set that can be used to train and assess a ReaxFF force field. During the training procedure, if a certain reaction or structure is observed in ReaxFF simulations which correspond to an entry in the data set, its validity can be assessed immediately instead of requiring an expensive DFT calculation. This will increase the efficiency of the training procedure.

Because ReaxFF does not have an implicit solvation model, it will be necessary to ensure that the behavior of HAN structures is correctly captured in both the gas phase and condensed phase. For an isolated HAN complex, this entails correct prediction of proton transfer based on the environment: in vacuum, the acid-base pair must be neutral NH_2OH and HNO_3 , while in solution, the ionic forms NH_3OH^+ and NO_3^- should be assumed. Obtaining precise energy differences between HAN structures as in Tables 1 and 2 is unnecessary in training, however, the ReaxFF force field should demonstrate that the structures are stabilized by hydrogen bonding.

ReaxFF will not train on every elementary reaction step in the detailed mechanism of HAN decomposition. Relative barrier heights for important pathways such as the autocatalytic pathway discussed in Section III.B must be qualitatively correct, however, so that the force field does not predict an alternative pathway which is known to be less energetically favorable. Even within a specific pathway, various isomerizations will lead to different barrier heights, making selection of data to include in a training set even more challenging. The ideal training set will create a force field which produces

Reaction	ΔE_f (kcal/mol)	ΔE_{rxn} (kcal/mol)
1	10.2	3.9
2	N/A	9.1
3	9.2	-11.5
4	17.0	-0.6
5	7.4	-28.9
6	N/A	8.9
7	15.0	4.9

Table 3 Barrier heights and energies of reaction (electronic) for steps in a HONO-regeneration pathway at the GIL/ ω B97X-D/6-311++G level of theory**

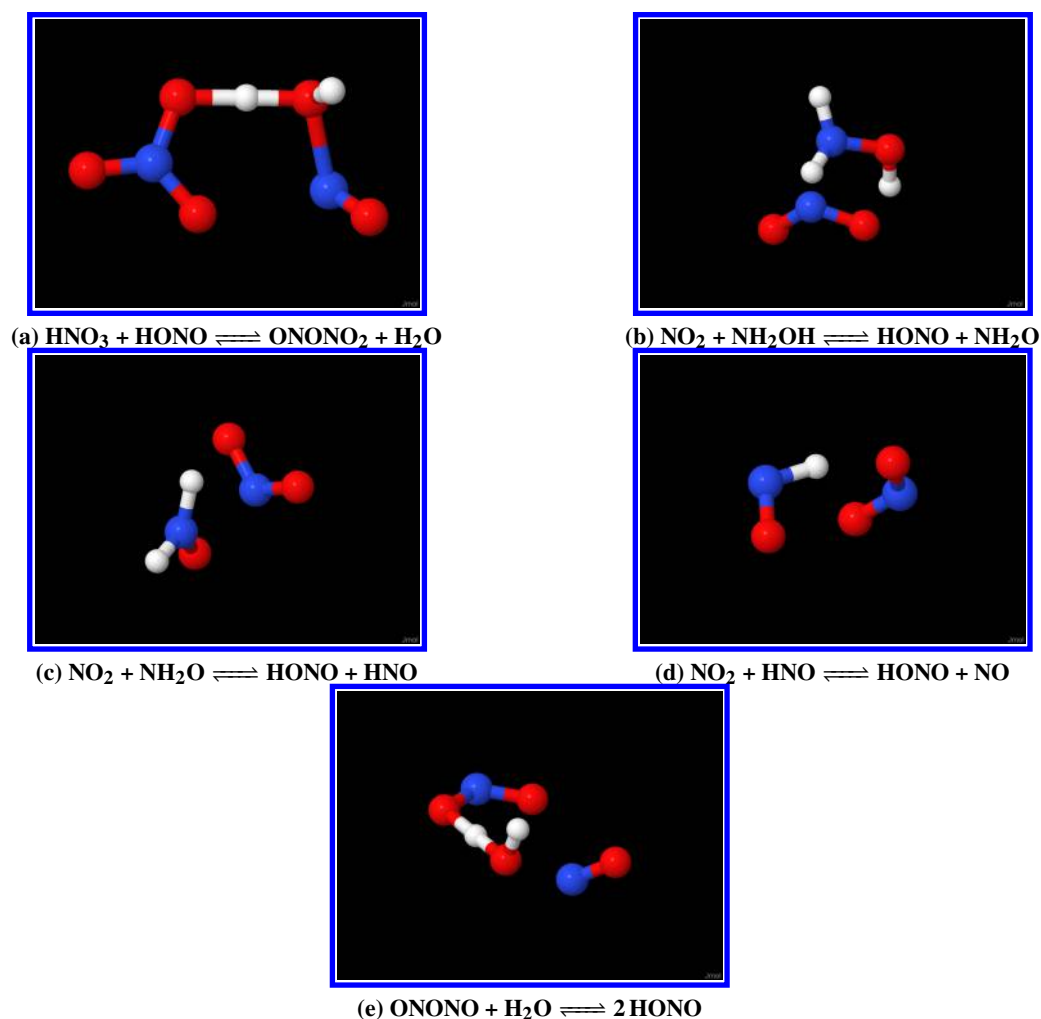


Fig. 5 Optimized condensed-phase geometries for transition states in a HONO-regeneration pathway at the GIL/ ω B97X-D/6-311++G** level of theory

relative energies of intermediates, products, and transition states in good agreement with reference DFT (or *ab initio*) data, while including as little of this reference data as possible.

References

- [1] Chambreau, S. D., Popolan-Vaida, D. M., Vaghjiani, G. L., and Leone, S. R., "Catalytic Decomposition of Hydroxylammonium Nitrate Ionic Liquid: Enhancement of NO Formation," *J. Phys. Chem. Lett.*, Vol. 8, No. 10, 2017, pp. 2126–2130. doi: 10.1021/acs.jpcclett.7b00672, URL <https://doi.org/10.1021/acs.jpcclett.7b00672>.
- [2] Klein, N., "Ignition and Combustion of the HAN-Based Liquid Propellants," The 27th JANNAF Combustion Subcommittee Meeting, 1990.
- [3] Rheingold, A. L., Cronin, J. T., Brill, T. B., and Ross, F. K., "Structure of hydroxylammonium nitrate (HAN) and the deuterium homolog," *Acta Cryst. C*, Vol. 43, No. 3, 1987, pp. 402–404. doi:10.1107/S0108270187095593, URL <https://doi.org/10.1107/S0108270187095593>.
- [4] Van Dijk, C. A., and Priest, R. G., "Thermal decomposition of hydroxylammonium nitrate at kilobar pressures," *Combustion and Flame*, Vol. 57, No. 1, 1984, pp. 15–24. URL <http://www.sciencedirect.com/science/article/pii/0010218084901330>.

- [5] Oxley, J. C., and Brower, K. R., "Thermal Decomposition Of Hydroxylamine Nitrate," 1988. doi:10.1117/12.943754, URL <https://doi.org/10.1117/12.943754>.
- [6] Lee, H., and Litzinger, T. A., "Chemical kinetic study of HAN decomposition," *Combustion and Flame*, Vol. 135, No. 1, 2003, pp. 151–169. URL <http://www.sciencedirect.com/science/article/pii/S0010218003001573>.
- [7] Raman, S., Ashcraft, R. W., Vial, M., and Klasky, M. L., "Oxidation of Hydroxylamine by Nitrous and Nitric Acids. Model Development from First Principle SCRF Calculations," *J. Phys. Chem. A*, Vol. 109, No. 38, 2005, pp. 8526–8536. doi:10.1021/jp053003c, URL <https://doi.org/10.1021/jp053003c>.
- [8] Izato, Y.-i., Koshi, M., Miyake, A., and Habu, H., "Kinetics analysis of thermal decomposition of ammonium dinitramide (ADN)," *Journal of Thermal Analysis and Calorimetry*, Vol. 127, No. 1, 2017, pp. 255–264. URL <https://doi.org/10.1007/s10973-016-5703-4>.
- [9] Zhang, K., and Thynell, S. T., "Thermal Decomposition Mechanism of Aqueous Hydroxylammonium Nitrate (HAN): Molecular Simulation and Kinetic Modeling," *J. Phys. Chem. A*, Vol. 122, No. 41, 2018, pp. 8086–8100. doi:10.1021/acs.jpca.8b05351, URL <https://doi.org/10.1021/acs.jpca.8b05351>.
- [10] van Duin, Adri C., T., Dasgupta, S., Lorant, F., and Goddard, W. A., "ReaxFF: A Reactive Force Field for Hydrocarbons," *J. Phys. Chem. A*, Vol. 105, No. 41, 2001, pp. 9396–9409. doi:10.1021/jp004368u, URL <https://doi.org/10.1021/jp004368u>.
- [11] Mortier, W. J., Ghosh, S. K., and Shankar, S., "Electronegativity-equalization method for the calculation of atomic charges in molecules," *J. Am. Chem. Soc.*, Vol. 108, No. 15, 1986, pp. 4315–4320. doi:10.1021/ja00275a013, URL <https://doi.org/10.1021/ja00275a013>.
- [12] Senftle, T. P., Hong, S., Islam, M. M., Kylasa, S. B., Zheng, Y., Shin, Y. K., Junkermeier, C., Engel-Herbert, R., Janik, M. J., Aktulga, H. M., Verstraelen, T., Grama, A., and van Duin, A. C. T., "The ReaxFF reactive force-field: development, applications and future directions," *Npj Computational Materials*, Vol. 2, 2016, p. 15011. URL <https://doi.org/10.1038/npjcompumats.2015.11>.
- [13] Mueller, J. E., van Duin, A. C. T., and Goddard, W. A., "Development and Validation of ReaxFF Reactive Force Field for Hydrocarbon Chemistry Catalyzed by Nickel," *J. Phys. Chem. C*, Vol. 114, No. 11, 2010, pp. 4939–4949. doi:10.1021/jp9035056, URL <https://doi.org/10.1021/jp9035056>.
- [14] Strachan, A., van Duin, A. C. T., Chakraborty, D., Dasgupta, S., and Goddard, W. A., "Shock Waves in High-Energy Materials: The Initial Chemical Events in Nitramine RDX," *Phys. Rev. Lett.*, Vol. 91, No. 9, 2003, p. 098301. URL <https://link.aps.org/doi/10.1103/PhysRevLett.91.098301>.
- [15] Fogarty, J. C., Aktulga, H. M., Grama, A. Y., van Duin, A. C. T., and Pandit, S. A., "A reactive molecular dynamics simulation of the silica-water interface," *J. Chem. Phys.*, Vol. 132, No. 17, 2010, p. 174704. doi:10.1063/1.3407433, URL <https://doi.org/10.1063/1.3407433>.
- [16] Strachan, A., Kober, E. M., van Duin, A. C. T., Oxgaard, J., and Goddard, W. A., "Thermal decomposition of RDX from reactive molecular dynamics," *J. Chem. Phys.*, Vol. 122, No. 5, 2005, p. 054502. doi:10.1063/1.1831277, URL <https://doi.org/10.1063/1.1831277>.
- [17] Chenoweth, K., van Duin, A. C. T., and Goddard, W. A., "ReaxFF Reactive Force Field for Molecular Dynamics Simulations of Hydrocarbon Oxidation," *J. Phys. Chem. A*, Vol. 112, No. 5, 2008, pp. 1040–1053. doi:10.1021/jp709896w, URL <https://doi.org/10.1021/jp709896w>.
- [18] Russo, M. F., Bedrov, D., Singhai, S., and van Duin, A. C. T., "Combustion of 1,5-Dinitrobiuret (DNB) in the Presence of Nitric Acid Using ReaxFF Molecular Dynamics Simulations," *J. Phys. Chem. A*, Vol. 117, No. 38, 2013, pp. 9216–9223. doi:10.1021/jp403511q, URL <https://doi.org/10.1021/jp403511q>.
- [19] Weismiller, M. R., Junkermeier, C. E., Russo, M. F., Salazar, M. R., Bedrov, D., and van Duin, A. C. T., "ReaxFF molecular dynamics simulations of intermediate species in dicyanamide anion and nitric acid hypergolic combustion," *Modelling and Simulation in Materials Science and Engineering*, Vol. 23, No. 7, 2015, p. 074007. URL <http://dx.doi.org/10.1088/0965-0393/23/7/074007>.
- [20] Schmidt, M. W., Baldrige, K. K., Boatz, J. A., Elbert, S. T., Gordon, M. S., Jensen, J. H., Koseki, S., Matsunaga, N., Nguyen, K. A., Su, S., Windus, T. L., Dupuis, M., and Montgomery Jr, J. A., "General atomic and molecular electronic structure system," *J. Comput. Chem.*, Vol. 14, No. 11, 1993, pp. 1347–1363. doi:10.1002/jcc.540141112, URL <https://doi.org/10.1002/jcc.540141112>.

- [21] Bernales, V. S., Marenich, A. V., Contreras, R., Cramer, C. J., and Truhlar, D. G., "Quantum Mechanical Continuum Solvation Models for Ionic Liquids," *J. Phys. Chem. B*, Vol. 116, No. 30, 2012, pp. 9122–9129. doi:10.1021/jp304365v, URL <https://doi.org/10.1021/jp304365v>.
- [22] Perdew, J. P., and Schmidt, K., "Jacob's ladder of density functional approximations for the exchange-correlation energy," *AIP Conference Proceedings*, Vol. 577, No. 1, 2001, pp. 1–20. doi:10.1063/1.1390175, URL <https://aip.scitation.org/doi/abs/10.1063/1.1390175>.
- [23] Chai, J.-D., and Head-Gordon, M., "Long-range corrected hybrid density functionals with damped atom–atom dispersion corrections," *Phys. Chem. Chem. Phys.*, Vol. 10, 2008, pp. 6615–6620. doi:10.1039/B810189B, URL <http://dx.doi.org/10.1039/B810189B>.
- [24] Zhao, Y., and Truhlar, D. G., "The M06 suite of density functionals for main group thermochemistry, thermochemical kinetics, noncovalent interactions, excited states, and transition elements: two new functionals and systematic testing of four M06-class functionals and 12 other functionals," *Theoretical Chemistry Accounts*, Vol. 120, No. 1, 2008, pp. 215–241. URL <https://doi.org/10.1007/s00214-007-0310-x>.
- [25] Kendall, R. A., Dunning, T. H., and Harrison, R. J., "Electron affinities of the first-row atoms revisited. Systematic basis sets and wave functions," *J. Chem. Phys.*, Vol. 96, No. 9, 1992, pp. 6796–6806. doi:10.1063/1.462569, URL <https://doi.org/10.1063/1.462569>.
- [26] Sun, H., and Vaghjiani, G. L., "Ab initio kinetics and thermal decomposition mechanism of mononitrobiuret and 1,5-dinitrobiuret," *J. Chem. Phys.*, Vol. 142, No. 20, 2015, p. 204301. doi:10.1063/1.4921378, URL <https://doi.org/10.1063/1.4921378>.
- [27] Spackman, M. A., "Potential derived charges using a geodesic point selection scheme," *J. Comput. Chem.*, Vol. 17, No. 1, 1996, pp. 1–18. doi:10.1002/(sici)1096-987x(19960115)17:1<1::aid-jcc1>3.0.co;2-v, URL [https://doi.org/10.1002/\(SICI\)1096-987X\(19960115\)17:1<1::AID-JCC1>3.0.CO;2-V](https://doi.org/10.1002/(SICI)1096-987X(19960115)17:1<1::AID-JCC1>3.0.CO;2-V).
- [28] Rigby, J., and Izgorodina, E. I., "Assessment of atomic partial charge schemes for polarisation and charge transfer effects in ionic liquids," *Phys. Chem. Chem. Phys.*, Vol. 15, No. 5, 2013, pp. 1632–1646. URL <http://dx.doi.org/10.1039/C2CP42934A>.
- [29] Alavi, S., and Thompson, D. L., "Hydrogen bonding and proton transfer in small hydroxylammonium nitrate clusters: A theoretical study," *J. Chem. Phys.*, Vol. 119, No. 8, 2003, pp. 4274–4282. doi:10.1063/1.1593011, URL <https://doi.org/10.1063/1.1593011>.

This article has been cited by:

1. Qingbo Zhu, Xiaoyang Lei, Bingzhi Liu, Zhihong Hu, Qiang Xu, Yang Pan, Baolin Hou, Xiaodong Wang, Zhandong Wang. 2024. Experimental and Theoretical Studies of HAN and HEHN Pyrolysis at Low Pressure. *Energy & Fuels* **38**:7, 6370-6378. [[Crossref](#)]
2. Helen J. Zeng, Thien Khuu, Steven D. Chambreau, Jerry A. Boatz, Ghanshyam L. Vaghjiani, Mark A. Johnson. 2020. Ionic Liquid Clusters Generated from Electrospray Thrusters: Cold Ion Spectroscopic Signatures of Size-Dependent Acid-Base Interactions. *The Journal of Physical Chemistry A* **124**:50, 10507-10516. [[Crossref](#)]